Computational design and preliminary experimental validation of a low-cost, structurally optimized rib cage surrogate

Katie R. G. Zilevicius[1], Tyler J. Roy[1], B. Wade von Kleeck[1], Brian Graybill[2], Jed Wilbur[2], F. Scott Gayzik[1], and Philip J. Brown[1],
[1] Wake Forest University School of Medicine; [2] Creare LLC

ABSTRACT

Primary Blast Injuries (PBIs) result from the interaction between high pressure blast waves and the air- and fluid-filled organs of the body. This includes, but is not limited to, pulmonary barotrauma or "blast lung." As modern-day military personal protective equipment (PPE) has evolved to improve blunt-force trauma survivability, higher numbers of Primary blast related injuries have been reported. Future efforts to create PBI-mitigating PPE will require novel tools and methodologies for evaluation. Current anthropometric test devices (ATDs) are designed for blunt-force testing and fabricated from high-durability materials lacking biofidelic representation of internal organs. This paper discusses the computational design and preliminary experimental validation of a novel, high-fidelity, low-cost rib cage surrogate for incorporation into a next-generation ATD for PBI risk assessment. Using a validated human body model for quantification of target chest behavior under key loading patterns, topology optimization was used to design a novel anatomically inspired design. Following fabrication of a physical prototype, experimental testing using a 6 degree of freedom robot was used to evaluate performance under point-loading across the ribcage. These values were compared to results of a cadaveric study previously used to validate the human body model from which the computational design is derived. Differences between the surrogate and cadaveric values were used to determine overall eligibility for incorporation into the novel blast ATD.

INTRODUCTION

Since the widespread introduction of explosives into modern warfare in World War I, exposure to blast has become one of the major sources of military casualties (Boutillier et al., 2022). To date, efforts to mitigate blast injuries have focused on the development of personal protective equipment (PPE) aimed at preventing penetrating (secondary) and blunt force (tertiary) traumatic injuries. As survivability from these injury forms has improved with advancements in PPE, higher numbers of primary blast injuries (PBIs), or injuries resulting from overpressure in the fluid-filled organs, are being reported (Moore et al., 2009; Phillips, 1986). PBIs include mild traumatic brain injury without physical head trauma, perforated bowels, ruptures of the tympanic membrane and ocular globe, and pulmonary barotrauma (Blast Injury Research Coordinating

This paper is a student paper from the 20th Injury Biomechanics Symposium and is published in a special issue of SAE International Journal of Transportation Safety.
It is preliminary work, has not been peer reviewed, and should not be cited because it is a work in progress.

Office, 2024). The severity of these injuries is often related to the magnitude of the blast and can range from mild to deadly (Argyros, 1997).

Future efforts to design PPE for the mitigation of PBI will require adaptation of the tools and methodologies currently used to evaluate PPE for secondary and tertiary blast injuries. To date, human body models (HBMs) have been used to successfully investigate PBI mechanisms, including thoracic injuries (Kirkman et al., 2011; MacFadden et al., 2012, Chanda et al., 2018). However, physical models are needed to examine the effects of novel PPE. Anthropometric test devices (ATDs) are critical tools for understanding injury mechanisms and evaluating the efficacy of PPE. However, current blast ATDs are fabricated from expensive, high durability materials with little to no representation of the internal organs making them better suited to secondary and tertiary blast injury detection. This work is part of an ongoing effort to develop a high-fidelity, low-cost blast ATD capable of providing accurate and easily interpretable data regarding PBI risk. This requires not only incorporation of phantom organs, but skeletal components that facilitate biofidelic transmission of pressure waves through the body.

This study aims to design and validate a structurally optimized rib cage surrogate to enable accurate organ-level measurements for prediction of thoracic PBIs such as pulmonary barotrauma. Based off published literature on injury risk curves for primary blast injuries to the lungs, bend sensors in the lateral ribs, accelerometers on the sternum, and embedded pressure sensors in the lungs will be used to identify percent chance of pulmonary barotrauma (MacFadden et al., 2012). As these sensing methods rely mechanical behavior of the ribcage, biofidelic response of this skeletal structure is crucial for accurate readings and injury risk prediction.

METHODS

The torso of the next-generational blast ATD will contain phantom organs, the ribcage, thoracic and lumbar spinal components, and an encapsulating “skin” layer of silicone. To capture biofidelic behavior, the rib cage surrogate will aim to encompass the mechanical response of the hard and soft tissue components of the chest wall. The final design must be a single, moldable unit tuned to fabrication with a low-cost off-the-shelf resin to keep costs at a minimum. The workflow in Figure 1 depicts the process developed herein.

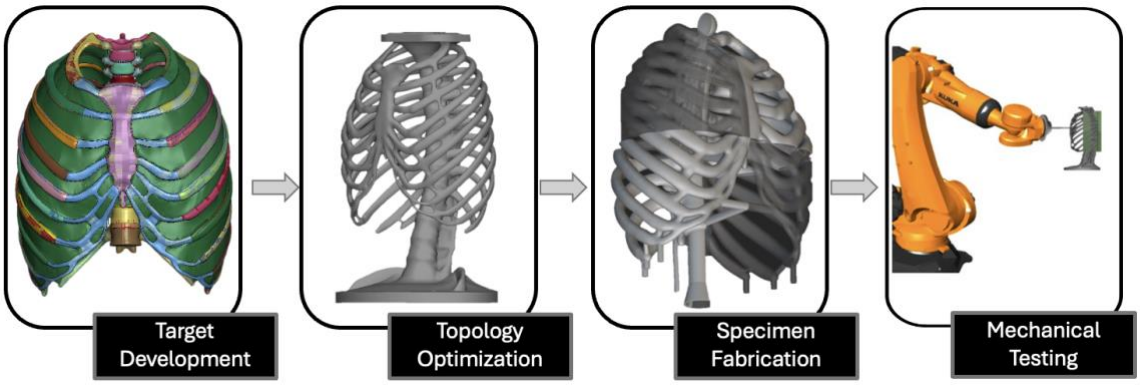

Figure 1: Workflow for ribcage design, fabrication, and validation.

This paper is a student paper from the 20th Injury Biomechanics Symposium and is published in a special issue of SAE International Journal of Transportation Safety.
It is preliminary work, has not been peer reviewed, and should not be cited because it is a work in progress.

Target Development

The ribs, joint capsules, costal cartilage, intercostal musculature, sternum, and thoracic spine and intervertebral discs were isolated from the Global Human Body Models Consortium (GHBMC) 50th percentile male detailed pedestrian model (M50). Using LS-Dyna, the spinal column was held stationary while load was applied to the sternum (0 degrees), oblique (45 degrees), and lateral (90 degrees) ribs, replicating military standard testing procedures for blast and ballistics PPE. Loads were applied in banded patterns to replicate pressure waves while remaining focused enough to prevent interference between loads during the design phase. Physiologically relevant loading values were determined based off prior cadaveric work by Kindig et al (2010).

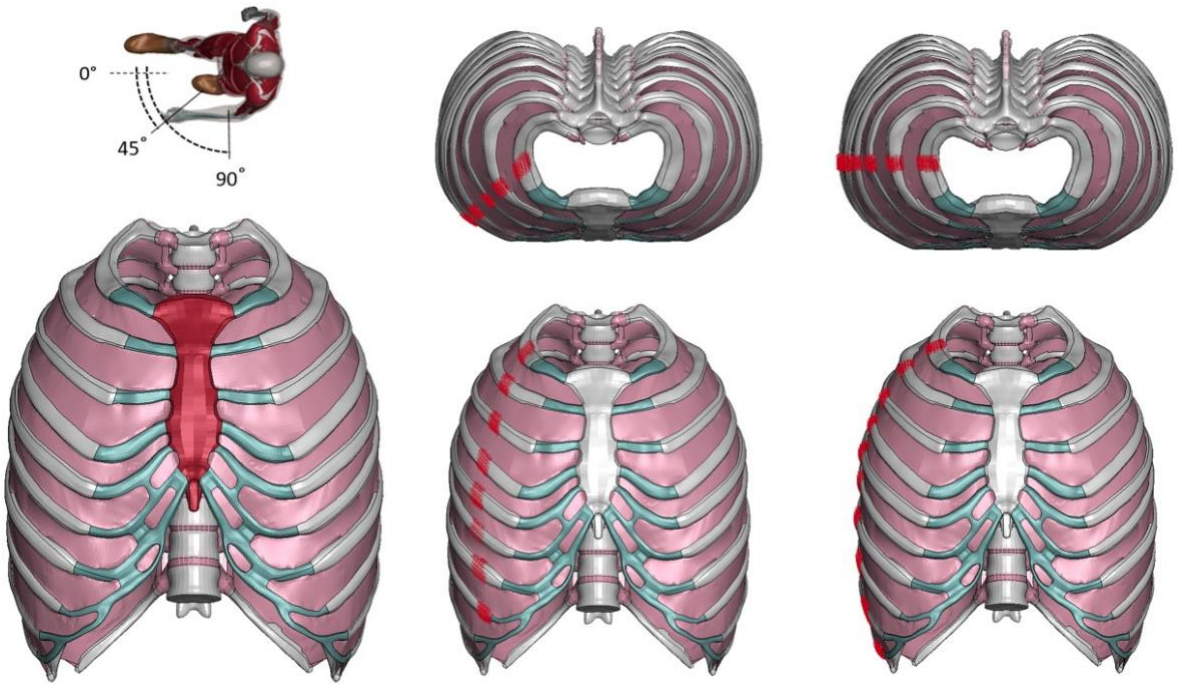

Figure 2: Simulation loading patterns at 0, 45, and 90 degrees.

Force-deflection data was collected for each simulation, and the area under each respective curve was calculated to determine elastic energy using Equation 1. The calculated elastic energy for each of the three simulations forms the design response target for each load case during the topology optimization phase.

$$E = \int_0^X F\, dx \qquad (1)$$

Topology Optimization

Topology optimization of the rib surrogate design was conducted using nTop (NY, USA), a computational design software. The GHBMC-M50 geometry was used to establish baseline anatomically inspired design regions for mechanical optimization. The passive design region was constructed by combining the ribs, sternum, and thoracic spine. This represents the minimum

This paper is a student paper from the 20th Injury Biomechanics Symposium and is published in a special issue of SAE International Journal of Transportation Safety.
It is preliminary work, has not been peer reviewed, and should not be cited because it is a work in progress.

volume core the optimization must maintain in the final design. The active design region surrounds the passive design region and represents the maximum working volume the optimization may operate within. This was defined by the outer boundary of the volume representing the complete chest wall using an expanded version of the rib geometry. The passive and active design regions can be seen in Figure 3.

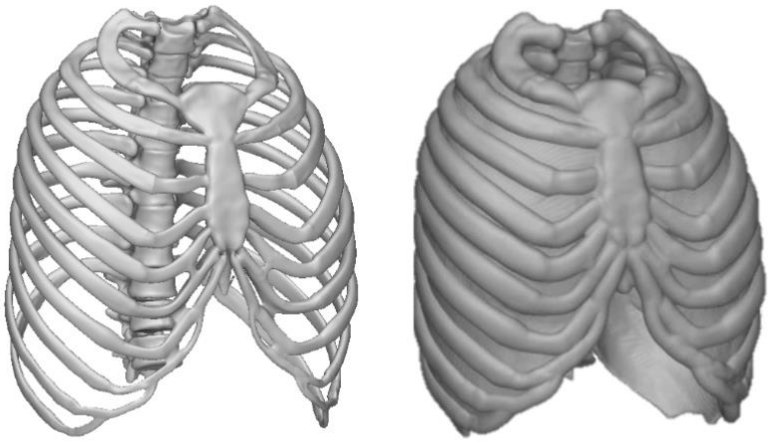

Figure 3. (Left) passive design region, (Right) active design region

Material selection was informed by the range of elastic modulus properties from tissue contained within the human chest wall. Using reported ranges of elastic moduli for cartilage in the thorax, materials reported to have an elastic modulus between 30 and 60 MPa were explored (Gradischar et al., 2022). An off-the-shelf-, urethane-based-, two-part resin, Flexane 80 (Devcon, USA) was selected for its elastic modulus (60 MPa), Poisson's ratio (0.35), and high-energy return ratio. These properties were provided to the optimization simulation.

The final component required for topology optimization is a set of constraints the optimization must aim to meet. These constraints are designed using the elastic energy calculations completed from the original GHBMC simulations. Replicating the loading bands at the sternum, oblique ribs, and lateral ribs from the original simulation, one constraint for each loading direction was created. Optimization simulations were run using a single (0 degree) and multi-directional (0, 45, and 90 degree) design response constraint. The computational design process iteratively applies the loading scenarios and mathematically determines optimal material placement to match the provided response. An additional constraint to enforce symmetry across the sagittal plane was leveraged to reduce computational expense.

Design simulations in nTop were run over 100-200 iterations under an overarching objective function. This objective function limits the simulation to designs falling between the passive and active design regions while attempting to converge on a design meeting all applied constraints. Iteration counts were monitored and adjusted as necessary to provide sufficient time for convergence to occur without excessive computational expense.

This paper is a student paper from the 20th Injury Biomechanics Symposium and is published in a special issue of SAE International Journal of Transportation Safety.
It is preliminary work, has not been peer reviewed, and should not be cited because it is a work in progress.

Specimen Fabrication

A custom four-part mold was designed for fabrication of a physical prototype by offsetting the outer boundary to form a shell whose internal volume matched the optimized design. With the addition of pour spouts and vacuum pull locations, a single-use mold was fabricated using a filament-based 3D printer (Bambu, Carbon, USA). Upon successfully printing each quadrant of the mold, all four sections were adhered using a two-part medical-grade epoxy (EA M-31CL, Loctite, USA) to form a single mold of the entire ribcage. Flexane 80 Liquid resin (Devcon, USA) was prepared in accordance with manufacturer instructions. Both Part A and Part B were warmed to 85°F before combining. After mixing, the resin was poured into the mold under vacuum pressure to prevent air bubbles. The mold was prepared with liquid mold release (Universal Mold Release, SmoothOn, USA) prior to pouring. Following a 16-hour cure time, the mold was removed and ribcage prototype made ready for testing.

Figure 4. Custom four-part mold design (left), 3D printed mold (center), and pouring of the Flexane under vacuum pressure (right).

Mechanical Testing

Previous work by Kindig et al (2010) evaluated the stiffness properties of the human ribcage at various locations. This cadaveric work was later used to validate the GHBMC M50 model. Validation testing of the surrogate prototype described below has been designed to replicate the original cadaveric work as closely as possible using a Kuka KR300 Ultra 6-degree-of-freedom robot outfitted with an Omega160 IP65 6 axis load cell (ATI, USA).

As in the original study, mounting methodology was designed to support the ribcage without impeding rib rotation. A custom 3D printed fixture was designed to interface with a standard 8020 Aluminum rail that forms the external wall of a permanent pedestal in the Kuka workspace. A comparison of the mounting methods in Kindig et al compared to this study can be found in Figure 5.

This paper is a student paper from the 20th Injury Biomechanics Symposium and is published in a special issue of SAE International Journal of Transportation Safety.
It is preliminary work, has not been peer reviewed, and should not be cited because it is a work in progress.

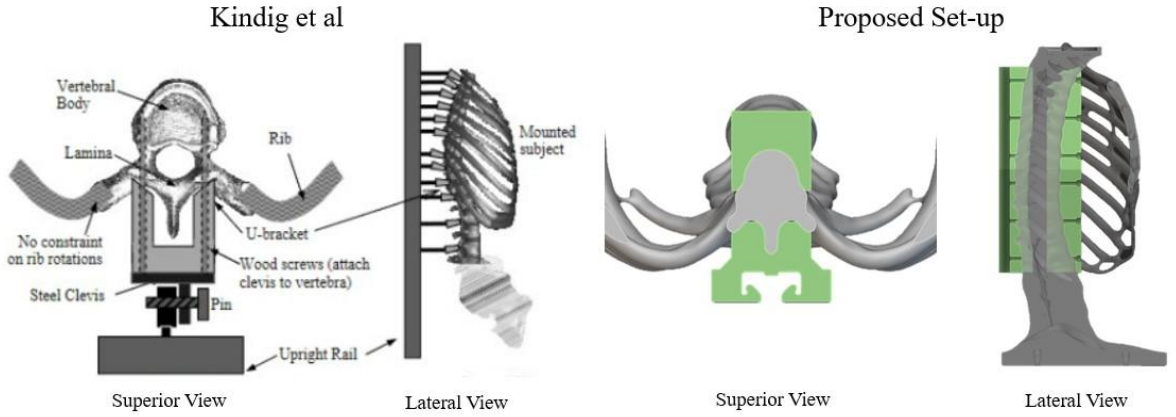

Figure 5. Comparison of mounting methodology between the original study by Kindig et al and this study.

Once mounted, Delrin spheres were attached to the surface of the ribcage using cyanoacrylate glue (Loctite, USA) to provide a frictionless surface for compression. A total of four locations were tested – the upper sternum, and the costal cartilage, costal cartilage junction, and bone of Rib 4 (Figure 6). Two sizes of Delrin spheres were cut to 40% depth; 19mm diameter spheres along the three Rib 4 locations, and a 25.4mm diameter sphere at the upper sternum were adhered with cyanoacrylate glue. To locate the spheres in space for compression by the Kuka robot, a 3D scanner (Peel3D, USA) was used to scan the entirety of the ribcage and pedestal. This scan was then used to generate custom trajectories for compression at all four testing locations using a Rhino3D and Grasshopper3D (TLM Inc, USA). Loading rates were programmed to match the original study, waveform to the plate, at a quasi-static rate (2 mm/sec). Force data from the ATI load cell time-synched to positional data from the Kuka robot were used to plot force deflection data. Data points were sampled every 4 milliseconds.

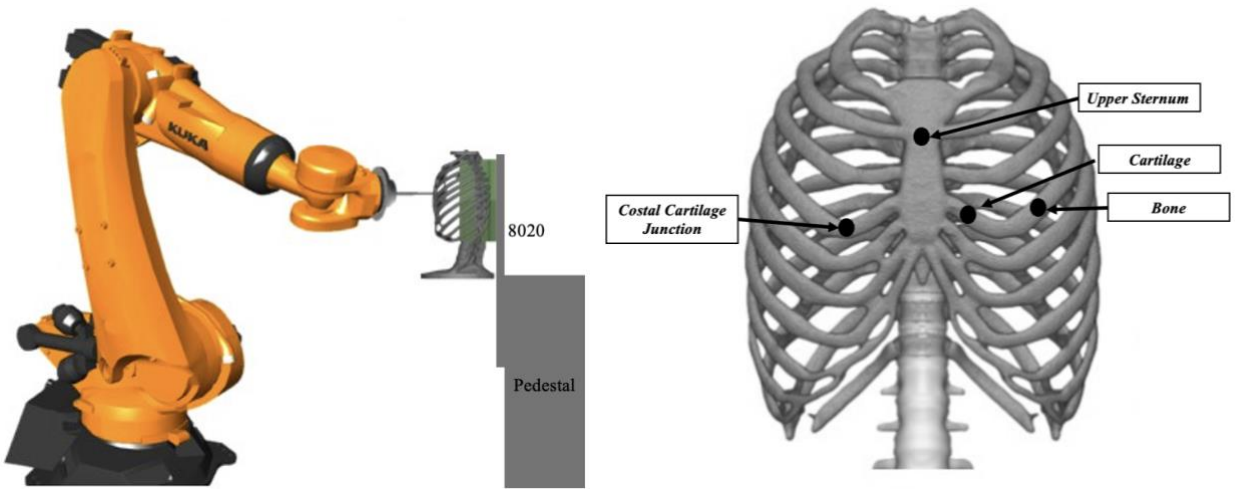

Figure 6: (Left) Mechanical testing set up, and (Right) sample testing locations

This paper is a student paper from the 20th Injury Biomechanics Symposium and is published in a special issue of SAE International Journal of Transportation Safety.
It is preliminary work, has not been peer reviewed, and should not be cited because it is a work in progress.

RESULTS

Topology Optimization

The optimization simulations for both the single and multi-directional cases were able to converge and generate designs, as seen in Figure 7. The single load case resulted in a heavily reinforced sternum and cartilage region. It also featured intercostal supports down the lateral rib and close to the spine. In the multi-directional design, a more uniform reinforcement all over the ribcage was observed, with similar connections between the ribs being observed at multiple locations. It is of note that the multi-directional load opted to retain the floating ribs and formed small connections between them.

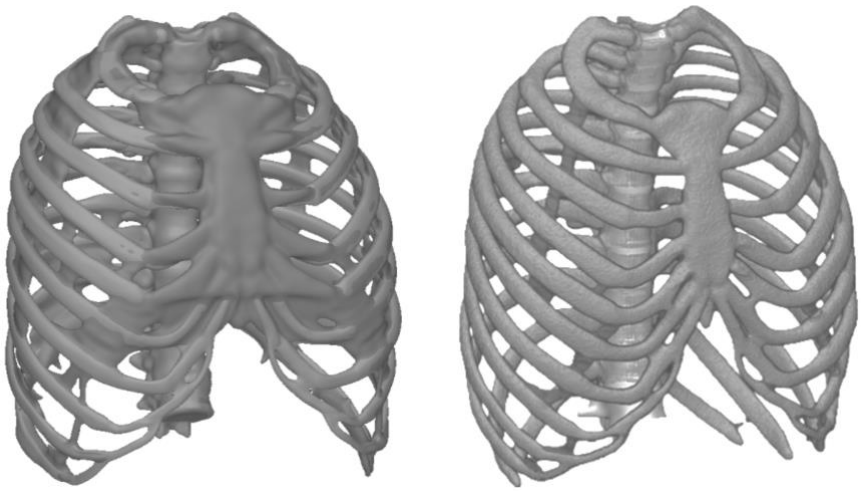

Figure 7. Optimization results for a single (left) and multi-directional (right) load cases.

Computational Validation

Following convergence on a design that met all prescribed criteria, the generated mesh designs were imported into LS-Dyna. Replication of the loading procedures described in the Target Development section was applied to the generated design for comparison of force-deflection response (Figure 8). Iterations of the design and computational validation process were repeated with adjustments to the design input factors until a final design with the ability to approach GHBMC behavior.

This paper is a student paper from the 20th Injury Biomechanics Symposium and is published in a special issue of SAE International Journal of Transportation Safety.
It is preliminary work, has not been peer reviewed, and should not be cited because it is a work in progress.

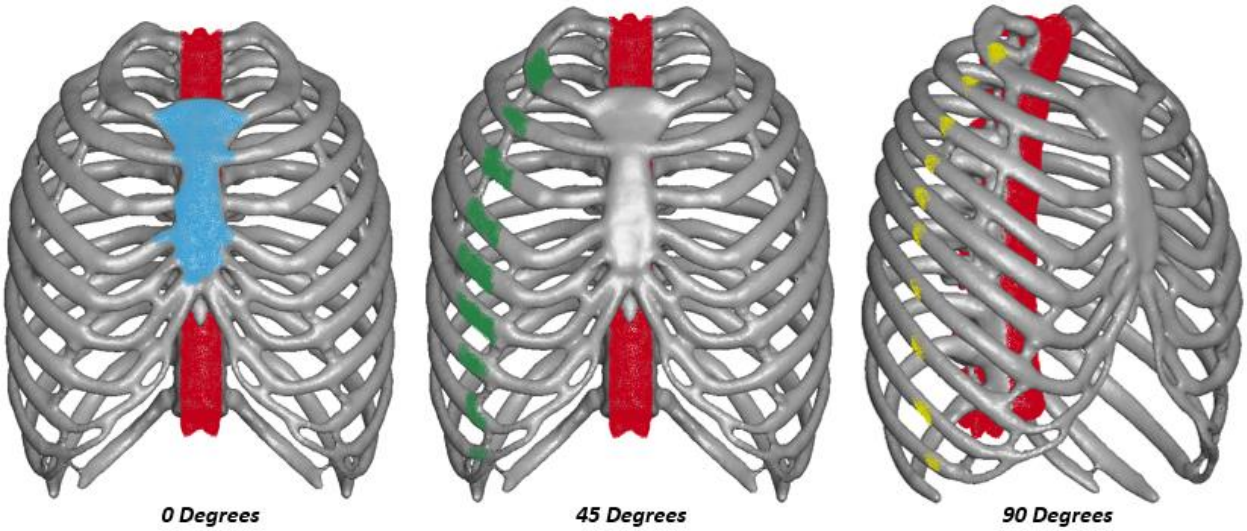

Figure 8. Simulation set up at (left to right) 0, 45, and 90 degrees for computational validation of generated designs. The red represents the stationary constraint on the thoracic spine.

The target deflection values for each load case can be found in Table 1. These represent the values obtained in the original GHBMC simulations. Resultant deflection for identical load cases is presented for the single and multi-directional optimized designs. While the multi-directional optimization simulation weighted each of the three directional constraints evenly, it performed best in the 0-degree loading condition. The multi-directional design performed superior to the single-direction design overall and was selected for fabrication and further testing.

Table 1: Deflection values for computational validation of the single and bi-directional load case designs compared to GHBMC-derived targets.

Load Case (Direction)	Target Deflection Values	Single Direction Optimization	Error (%)	Multi-Directional Optimization	Error (%)
0 Degrees	20 mm	12.5 mm	19.38	20 mm	0.0
45 Degrees	10 mm	1.5 mm	85	6.7 mm	33.0
90 Degrees	2.3 mm	1 mm	56.52	1 mm	56.52

Specimen Fabrication

After the complete 16-hour cure time, the mold was destructively removed. Following complete removal of all PLA mold components, the specimen was allowed to continue curing. Mechanical testing occurred 6 days post-pour. Figure 9 displays the final molded prototype with and without the Delrin spheres.

This paper is a student paper from the 20th Injury Biomechanics Symposium and is published in a special issue of SAE International Journal of Transportation Safety.
It is preliminary work, has not been peer reviewed, and should not be cited because it is a work in progress.

Figure 9. Casted prototype (left, center) mounted with Delrin spheres (right).

Mechanical Testing

Four locations of the 27 originally tested by Kindig et al were selected for mechanical testing. Force deflection data was collected at the Upper Sternum, Rib 4 Cartilage, Rib 4 Costal Cartilage Junction, and Rib 4 Bone. Depth targets were designed to match the those seen at each location in the Kindig study. Data collection at the Upper Sternum was terminated early due to the end effector slipping off the surface of the Delrin sphere at that location. All other locations were successfully tested to their prescribed depth targets.

Data was brought into MATLAB (Mathworks, USA) for processing and plotting. Each compression was isolated for independent processing. Using the independent signals collected for force in X, Y, and Z by the ATI loadcell, a resultant force was calculated. This resultant was zeroed at the start of the compression to provide information on net change in force. Similarly, position data for X, Y, and Z provided by the Kuka robot were used to determine resultant deflection which was zeroed at the same frame as the time-synched force data.

For comparison, the plots provided by Kindig et al were digitized using the Graph Digitizer tool (version 1.3.1, Andrey Shapkin). At each location tested by Kindig et al, three data traces are reported – one for each of the three postmortem human subjects (PMHS) evaluated. The force deflection curves for each subject at each of the four testing locations repeated here were digitized to form a range and "average" human response seen in Figure 10.

This paper is a student paper from the 20th Injury Biomechanics Symposium and is published in a special issue of SAE International Journal of Transportation Safety.
It is preliminary work, has not been peer reviewed, and should not be cited because it is a work in progress.

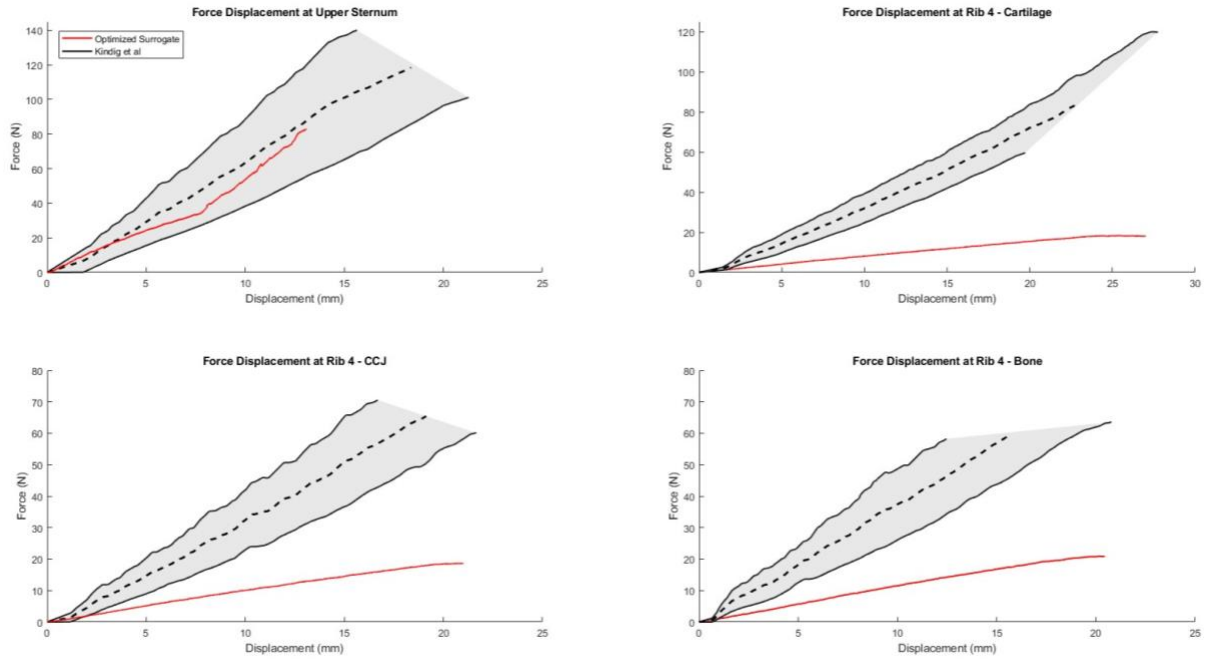

Figure 10. Mechanical testing data

Prior to the early termination of the Upper Sternum test, the surrogate ribcage replicated the PMHS data well by remaining within the bounds shown. At the three other testing locations, higher frequencies of deviation from the PMHS corridor were apparent. Maximum force for the surrogate compared to average maximum for the PMHS data at matched deflection values can be seen in Table 2.

Table 2: Maximum force values for each testing location compared to the "average" maximum force from PMHS data at matched deflection. *Upper Sternum test terminated early

Location	Deflection (mm)	PMHS Force (N)	Surrogate Force (N)	Error (%)
Upper Sternum	18.36	95.16	82.61*	13.18*
Rib 4 - Cartilage	22.64	82.84	17.24	79.18
Rib 4 - CCJ	19.13	65.46	17.89	72.67
Rib 4 - Bone	16.70	50.53	14.93	70.45

DISCUSSION

This work aimed to replicate the multi-directional behavior of the GHBMC M50 chest wall in a novel ribcage surrogate created through topology optimization. Using design response constraints derived from simulations of the GHBMC M50, computational design software was able to generate designs using information regarding a low-cost, off-the-shelf fabrication material.

This paper is a student paper from the 20th Injury Biomechanics Symposium and is published in a special issue of SAE International Journal of Transportation Safety.
It is preliminary work, has not been peer reviewed, and should not be cited because it is a work in progress.

Key takeaways from the topology optimization section of this work include that the incorporation of multi-directional loading cases improves the resulting design's ability to mimic the human chest wall. It is hypothesized that additional information on response behavior influences optimal choices in material placement. However, as more loads are included, the more difficult and computationally expensive topology optimization becomes.

Specimen fabrication methods used in this preliminary study are not representative of production-quality techniques. Multi-use molds are costly and typically created from milled aluminum. This study aimed to preliminarily assess mechanical behavior of the topology optimized design before proceeding with such an expense.

Looking at the percent error in the computational validation, the Upper Sternum was expected to outperform the other locations. Under simulated conditions, the Upper Sternum location matched the performance of the GHBMC with perfect accuracy. During experimental conditions, the Upper Sternum force deflection tracked nearly identical to the average PMHS response prior to its early termination. Adjustment of the trajectory paired with a larger end effector will be explored in future tests to prevent early termination. Room for improvement at the three Rib 4 testing locations remains. Opposing trends during performance under computational and experimental testing at these locations were apparent. In simulation, error increased farther from the sagittal plane; experimentally the opposite was true with the most lateral location (bone) performing closest to its target.

Future iterations of both the design and fabrication material will be explored. Using the experimental data collected in this study, updates to the design response targets can be made. Through continued comparison of experimental surrogate data to the original Kindig cadaveric data, an understanding of the surrogate's ability to replicate human behavior under quasistatic loading conditions can be obtained. Once an optimal design and material have been selected, high durability, multi-use molds will be obtained for integration of the design into the torso simulator. Upon completion, field tests under blast conditions would be completed. The authors propose future investigation into the surrogate response BioRank, CORA, and ISO standards relating to biofidelity and similarity scoring.

CONCLUSIONS

This work aimed to design and validate a low-cost, biofidelic rib cage for use in highly destructive testing scenarios where frequent replacement is necessary. Through the application of topology optimization, the novel workflow developed herein attempted to harness the biofidelic behavior of the GHBMC M50 chest wall. By optimizing the design to achieve compliance on par with the human chest wall, future data collected will yield more accurate injury risk predictions. Preliminary computational validation indicated a computational design derived from multi-directional loads as viable for fabrication. Experimental testing of the prototype yielded high accuracy performance at the sternum, with the need for additional work to improve loading at various locations across the ribs before incorporation into a novel blast ATD.

This paper is a student paper from the 20th Injury Biomechanics Symposium and is published in a special issue of SAE International Journal of Transportation Safety.
It is preliminary work, has not been peer reviewed, and should not be cited because it is a work in progress.

ACKNOWLEDGEMENTS

This research is supported by U.S. Army Medical Research Acquisition Activity under contract # HT942523C0053. The views, opinions and/or findings contained in this abstract are those of the author(s) and should not be construed as an official Department of the Army position, policy or decision unless so designated by other documentation.

The authors would like to thank the supporting team members from Creare LLC and Wake Forest University School of Medicine for their assistance in the larger project aiming to develop and test the novel blast ATD.

REFERENCES

ARGYROS, G. J. (1997). Management of Primary Blast Injury. Toxicology, 121 (1), 105-115.

BLAST INJURY RESEARCH COORDINATING OFFICE. (2024). What is Blast Injury? U.S. Department of Defense. Available online at: https://blastinjuryresearch.health.mil/index.cfm/blast_injury_101

BOUTILLIER, J., CARDONA, V., MAGNAN, P., OGIER, M., DE MEZZO, S., MONTESPAN, F., MENINI, W., MOSNIER, J., NAZ, P., PRAT, N. (2022). A New Anthropometric Mannequin for Efficacy Evaluation of Thoracic Protective Equipment Against Blast Threats. Frontiers in Bioengineering and Biotechnology, 9, 7786881.

CHANDA, A., CALLAWAY, C. (2018). Computational Modeling of Blast Induced Whole-Body Injury: A Review. Journal of Medical Engineering & Technology, 42 (2), 88-104.

GRADISCHAR, A., LEBSCHY, C., KRACH, W., KRALL, M., FEDIUK, M., GIERINGER, A., SMOLLE-JÜTTNER, F., HAMMER, N., BEYER, B., SMOLL, J., SCHÄFER, U. (2022). Measurement of Global Mechanical Properties of Human Thorax: Costal Cartilage. Journal of Biomechanics, 142, 111242.

KINDIG, M., LAU, A., FORMAN, J., KENT, R. (2010). Structural Response of Cadaveric Ribcages Under Localized Loading: Stiffness and Kinematic Trends. Stapp Car Crash Journal, 54, 337-380.

KIRKMAN, E., WATTS, S., COOPER, G. (2011). Blast Injury Research Models. Philosophical Transactions of the Royal Society B: Biological Sciences, 366, 144-159.

MACFADDEN, L., CHAN, P., HO, K., STUHMILLER, J. (2012). A Model for Predicting Primary Blast Lung Injury. The Journal of Trauma and Acute Care Surgery, 73 (5), 1121-1129.

MOORE, D., JERUSALEM, A., NYEIN, M., NOELS, L., JAFEE, M., RADOVITZKY, R. (2009). Computational Biology – Modeling of Primary Blast Effects on the Central Nervous System. NeuroImage, 47, T10-T20.

PHILLIPS, Y. Y. (1986). Primary Blast Injuries. Annals of Emergency Medicine, 15 (12), 1446-1450.

This paper is a student paper from the 20th Injury Biomechanics Symposium and is published in a special issue of SAE International Journal of Transportation Safety.
It is preliminary work, has not been peer reviewed, and should not be cited because it is a work in progress.